

Peristaltic Flow of a Fluid in a Porous Channel: a Study Having Relevance to Flow of Bile Within Ducts in a Pathological State

S. Maiti^{1*}, J. C. Misra^{2†}

¹*School of Medical Science and Technology & Centre for Theoretical Studies,
Indian Institute of Technology, Kharagpur, India*

²*Department of Mathematics, Institute of Technical Education & Research,
Siksha 'O' Anusandhan University, Bhubaneswar, India*

Abstract

The paper deals with a theoretical study of the transport of a fluid in a channel, which takes place by the phenomenon of peristalsis. A mathematical analysis of the said problem has been presented. The analysis involves the application of a suitable perturbation technique. The velocity profile and the critical pressure for the occurrence of reflux are investigated with particular emphasis by using appropriate numerical methods. The effects of various parameters, such as Reynolds number, pressure gradient, porosity parameter, Darcy number, slip parameter, amplitude ratio and wave number on velocity and critical pressure for reflux are investigated in detail. The computed results are compared with a previous analytical work and an experimental investigation reported earlier in existing scientific literatures. The results of the present study are in conformity to both of them. The study has got some relevance to the physiological flow of bile in the common bile duct in a pathological state. It reveals that in the presence of gallstones, bile velocity increases as the value of the porosity parameter increases, while the critical pressure for reflux decreases as porosity increases.

Keywords: Peristaltic Transport, Darcy Number, Porosity, Velocity Profile, Critical Pressure.

*Email address: somnathm@cts.iitkgp.ernet.in (*S. Maiti*)

†Email address: misrajc@rediffmail.com; jcm@maths.iitkgp.ernet.in (*J.C.Misra*)

1 Introduction

Peristaltic pumping [1, 2] of physiological fluids induced by a progressive wave of area contraction or expansion along the length of a distensible tube has drawn serious attention of researchers working in the area of physiological fluid dynamics. Movement of various physiological fluids, such as the transport of urine from the kidney to the bladder through ureters, movement of food material through the digestive tract, transport

Nomenclature

a	Traveling wave amplitude
c_{20}, c_{21}, c_{22}	Integration constants
d	Half width of mean spacing between solid boundaries
D	Constant defined in equation (34)
$f(y)$	Function defined in equation (35)
k	Permeability parameter/Darcy number
p	Fluid pressure
$\frac{\partial p}{\partial x}$	Pressure gradient averaged over a period of time
R	Reynolds number of the fluid
s	Slip parameter at the boundary
t	Time
u, v	Velocity components in X and Y directions respectively
x, y	Rectangular Cartesian co-ordinates
α	Wave number
β	Complex number defined in equation (31)
e	Porosity parameter
λ	Wave length of the travelling wave motion of the wall
μ	Dynamic viscosity of the fluid
μ_1	Apparent viscosity of the fluid
ϕ	Phase difference
ρ	Density of the fluid
$\phi_1, \phi_{20}, \phi_{22}$	Functions defining ψ_1, ψ_2 in equation (20) and (21) respectively
ψ	Stream function
ϵ	Amplitude ratio
η	Vertical displacements of the wall

of semen in the vas deferens, movement of lymphatic fluids in lymphatic vessels, flow of bile (cf. Daniel et al. [3]) from gall bladder into the duodenum, spermatozoa in the ductus deferens of the male reproductive tract and cervical canal, movement of ovum in the fallopian tube as well as the cilia movement and circulation of blood in small blood vessels, — are all performed by the mechanism of peristalsis. The propulsion of some industrial fluids are take place by this mechanism. Peristaltic transport has also found various applications in roller and finger pumps, heart-lung machines, blood pump machines, dialysis machines and also transport of noxious fluid in nuclear industries.

A few theoretical studies on peristaltic transport of different physiological fluids were carried out by Usha and Rao [4], Mishra and Rao [5, 6], Misra et al [7, 8, 9, 10, 11, 12], as well as Eytan et al. [13]. The analyses were mostly restricted to consideration of small peristaltic wave amplitude and the assumption that the fluid inertia is negligible.

Taylor [14] conducted an investigation on asymmetric wave propagation in wavy sheets with the main objective of deriving some information regarding the mechanical interaction between spermatozoa. In order to study some fluid dynamical aspect of the problem of peristaltic transport in an asymmetric channel under Stokes flow conditions, the boundary integral method along with a suitable numerical technique was employed by Pozrikidis [15]. Using the assumptions of thin shell and lubrication theories, Carew and Pedley [16] put forward a mathematical analysis for the development of peristaltic pumping in the ureter by using similar assumptions. By taking into account the wall deformation of the pipe, Antanovskii and Ramkissoon [17] also used lubrication theory in order to analyse the peristaltic motion of a compressible viscous fluid through a pipe for situations where the pressure drop changes with time.

Bile (alternatively called as gall) is a greenish yellow secretion that contains various biochemical substances like bile acids, bile salts, pigments, cholesterol, phospholipids and electrolytic chemicals. Bile is produced in the liver. In adult humans, the quantity produced in a day is about one litre. After passing through several bile ducts, which penetrate the liver, bile flows into to the the common bile duct. It helps accelerate the fat absorption process and there by plays an important role in absorbing the vitamins D, E, K and A that are soluble in fat.

It has been suggested by recent physiological researchers (cf. Vries et al.[18]) that uterine peristalsis resulting from myometrial contraction can take place in both symmetric and asymmetric directions. Various investigators have carried out different studies pertaining to the gastrointestinal tract, intra-pleural membranes, capillary walls, human lung, bile duct, gall bladder with stones and small blood vessels, as well as flow in porous tubes and deformable

porous layers. Keener and Sneyd [19] reported that gastrointestinal tract is surrounded by a number of heavily innervated muscle layers which are smooth muscles consisting of many folds. There exist pores in the junctions between them, although the junctions are tight. As mentioned by Bergel [20], the capillary walls are surrounded by flattened endothelial cell layers, which are porous. Li et al. [21] reported that an impulsive magnetic field can be used as a therapeutic means to treat patients who have stone fragments in their urinary tract.

Functions of the human biliary system that consists of an organ and a ductal system are to create, transport, store as well as release bile into the duodenum to assist digestion of fats. This system contains the liver, gallbladder and biliary tract namely cystic, hepatic and common bile ducts. Although several analytical and physiological aspects of the human biliary system have been analyzed elaborately, we have only insufficient information about the mechanism of bile flow in the system. Torosoli and Ramorino [22] reported that pressures in the biliary tree vary from 0-14 cm H_2O (1 cm H_2O = 100 Pa) in the resting gall bladder to approximately 12-20 cm H_2O in the common bile duct.

Cholelithiasis is a disease that concerns formation of Gallstones. It has become a major health problem worldwide, particularly in adult population. Incidence of the gallstone disease indicates considerable geographical and regional variations [23, 24, 25, 26, 27, 28].

Lauga and Stone [29] made an experimental attempt to evaluate the effective slip length of the resulting flow as a function of the degrees of freedom describing the surface heterogeneities, namely the relative width of the no-slip and no-shear stress regions and their distribution along the pipe. They gave a possible interpretation of the experimental results which is consistent with a large number of distributed slip domains such as nano-size and micron-size nearly flat bubbles coating the solid surface. In addition they also suggested that the possibility of a shear-dependent effective slip length.

There are, however, only a few studies on the rheological properties of human bile. Gottschack and Lochner [30] examined 33 samples and reported that post-operative T-tube human bile is a Maxwell fluid. Coene et al. [31] claimed that 11 of 36 hepatic bile samples displayed non-Newtonian behaviour. Lou et al. [32] suggested on the basis of their preliminary measurements of fresh human bile collected at 37°C for a healthy person without gallstones that bile is a Newtonian fluid.

From the physiological fluid dynamics point of view, we present here a theoretical study that has relevance to the problem of bile transport in the common bile duct in the presence of stones. Peristaltic transport of the fluid in a porous channel has been investigated. The symmetric

sinusoidal peristaltic wave train on the channel walls, impermeable boundary and slip boundary condition of Saffman type have been considered in this study. The overall aim of the study has been to examine the role of fluid dynamics in the human biliary system, in particular for flow in a common bile duct with/without stones. It is expected that the results presented here will serve as fairly good theoretical estimates of various prospective fluid mechanical flow governing parameters related to the peristaltic transport of bile.

2 Problem Formulation

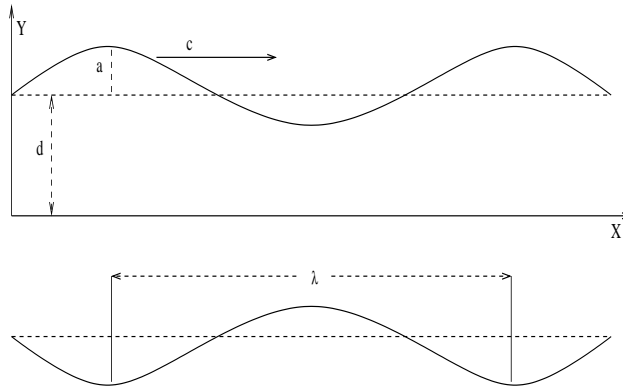


Fig. 1: Geometry of the problem

In a pathological state, numerous stones are formed in the bile (physiological fluid). In such a situation the mixture of the fluid (bile) and the solid particles (stones) forms a dense porous mass. We are interested here to study the motion of such a fluid (dense mixture), by considering it as a porous mass and treating it as an incompressible viscous fluid. Slip boundary conditions of Saffman's type have been considered in the study. We use Cartesian coordinates (x,y) , where x is measured in the direction of wave propagation and y in the direction normal to the mean position of the corresponding common bile duct (cf. Fig.1). Let u, v denote the velocity components in the directions of increasing x and y respectively; ρ, p, ν and t stand for the density, pressure, kinematic viscosity of the fluid and time respectively. A sinusoidal wave train is propagating with a constant speed c along the channel wall, such that $\eta = a \cos(\frac{2\pi}{\lambda}(x - ct))$ where $y = d + \eta$ and $y = -d - \eta$ represent the upper and lower boundaries of the channel and a is the wave amplitude, λ the wave length, $2d$ the width of the channel.

In order to study the motion of the fluid in the porous structure, we make use of Brinkman's

equations. These equations and the equation of continuity may be put as

$$\rho \left(\frac{\partial u}{\partial t} + u \frac{\partial u}{\partial x} + v \frac{\partial u}{\partial y} \right) = - \frac{\partial p}{\partial x} + \mu_1 \left(\frac{\partial^2 u}{\partial x^2} + \frac{\partial^2 u}{\partial y^2} \right) - \frac{\mu}{k} u \quad (1)$$

$$\rho \left(\frac{\partial v}{\partial t} + u \frac{\partial v}{\partial x} + v \frac{\partial v}{\partial y} \right) = - \frac{\partial p}{\partial y} + \mu_1 \left(\frac{\partial^2 v}{\partial x^2} + \frac{\partial^2 v}{\partial y^2} \right) - \frac{\mu}{k} v \quad (2)$$

$$\frac{\partial u}{\partial x} + \frac{\partial v}{\partial y} = 0 \quad (3)$$

where $\mu_1 = \frac{\mu}{e}$ and e, k are respectively the porosity, permeability parameters.

Introducing the stream function ψ , we write

$$u = \frac{\partial \psi}{\partial y}, \quad v = - \frac{\partial \psi}{\partial x}.$$

Eliminating p , one can write the equation that governs the flow of the fluid in terms of ψ in the following form :

$$\begin{aligned} \psi_{t_{yy}} + \psi_{t_{xx}} + \psi_y \psi_{y_{yy}} - \psi_x \psi_{y_{yy}} + \psi_y \psi_{x_{xx}} - \psi_x \psi_{x_{xx}} &= \frac{\nu}{e} (\psi_{yyyy} + 2\psi_{xxyy} + \psi_{xxxx}) \\ &- \frac{\nu}{k} \psi_{yy} - \frac{\nu}{k} \psi_{xx}, \text{ in which } \nu = \frac{\mu}{\rho} \end{aligned} \quad (4)$$

In the sequel, we shall use the following non-dimensional variables defined by

$$\begin{aligned} \bar{x} &= \frac{x}{d}, \quad \bar{y} = \frac{y}{d}, \quad \bar{u} = \frac{u}{c}, \quad \bar{v} = \frac{v}{c}, \quad \epsilon = \frac{a}{d}, \quad \bar{p} = \frac{p}{\rho c^2}, \quad \bar{t} = \frac{ct}{d}, \quad \bar{\eta} = \frac{\eta}{d}, \\ R &= \frac{cd}{\nu}, \quad \bar{\psi} = \frac{\psi}{cd}, \quad \bar{k} = \frac{k}{d^2}, \quad \alpha = \frac{2\pi d}{\lambda} \end{aligned} \quad (5)$$

If we now drop bars over the symbols, equation (4) may be expressed as

$$\begin{aligned} R(\psi_{t_{yy}} + \psi_{t_{xx}} + \psi_y \psi_{y_{yy}} - \psi_x \psi_{y_{yy}} + \psi_y \psi_{x_{xx}} - \psi_x \psi_{x_{xx}}) &= \frac{1}{e} (\psi_{yyyy} + 2\psi_{xxyy} + \psi_{xxxx}) \\ &- \frac{1}{k} \psi_{yy} - \frac{1}{k} \psi_{xx} \end{aligned} \quad (6)$$

2.1 Boundary Conditions

Let us now consider the symmetric motion of the flexible walls. The boundary conditions for the present problem may be stated as follows :

- (i) *non zero velocity slip of Saffman type* : $u = \mp s u_y$ or $\psi_y = \mp s \psi_{yy}$ at $y = \pm d \pm \eta$
 - (ii) *symmetric motion of the wall* : $v = \pm \frac{\partial \eta}{\partial t}$ or $-\psi_x = \pm \frac{2\pi ac}{\lambda} \sin \left(\frac{2\pi}{\lambda} (x - ct) \right)$ at $y = \pm d \pm \eta$
- (7)

3 Solution Procedure

In order to solve the governing equation along with the boundary conditions, let us express the stream function ψ as a power series in terms of amplitude ratio ϵ (considered as a small quantity), as follows :

$$\psi = \psi_0 + \epsilon\psi_1 + \epsilon^2\psi_2 + \dots \quad (8)$$

Similarly, we write the pressure gradient $\frac{\partial p}{\partial x}$ as

$$\frac{\partial p}{\partial x} = \left(\frac{\partial p}{\partial x}\right)_0 + \epsilon \left(\frac{\partial p}{\partial x}\right)_1 + \epsilon^2 \left(\frac{\partial p}{\partial x}\right)_2 + \dots \quad (9)$$

In equation (9) the first term on the right corresponds to an imposed pressure gradient, while the higher order terms are conceived of as those arising out of the peristaltic mechanism. Substituting (8) into (6), equating the coefficients of like powers of ϵ and neglecting cubes and higher power of ϵ , we get

$$\frac{\partial}{\partial t} \nabla^2 \psi_0 + \psi_{0y} \nabla^2 \psi_{0x} - \psi_{0x} \nabla^2 \psi_{0y} = \frac{1}{eR} \nabla^2 \nabla^2 \psi_0 - \frac{1}{kR} \nabla^2 \psi_0 \quad (10)$$

$$\frac{\partial}{\partial t} \nabla^2 \psi_1 + \psi_{1y} \nabla^2 \psi_{0x} + \psi_{0y} \nabla^2 \psi_{1x} - \psi_{1x} \nabla^2 \psi_{0y} - \psi_{0x} \nabla^2 \psi_{1y} = \frac{1}{eR} \nabla^2 \nabla^2 \psi_1 - \frac{1}{kR} \nabla^2 \psi_1 \quad (11)$$

$$\frac{\partial}{\partial t} \nabla^2 \psi_2 + \psi_{2y} \nabla^2 \psi_{0x} + \psi_{1y} \nabla^2 \psi_{1x} + \psi_{0y} \nabla^2 \psi_{2x} - \psi_{2x} \nabla^2 \psi_{0y} - \psi_{1x} \nabla^2 \psi_{1y} - \psi_{0x} \nabla^2 \psi_{2y} = \frac{1}{eR} \nabla^2 \nabla^2 \psi_2 - \frac{1}{kR} \nabla^2 \psi_2 \quad (12)$$

in which $\nabla^2 = \frac{\partial^2}{\partial x^2} + \frac{\partial^2}{\partial y^2}$ and $\psi_{ix} = \frac{\partial \psi_i}{\partial x}$, $\psi_{iy} = \frac{\partial \psi_i}{\partial y}$, $i = 0, 1, 2$.

Substituting of (8) into (7), we obtain the following boundary conditions by equating the coefficients of like power of ϵ .

$$\psi_0(\pm 1) = 0 \quad \text{and} \quad \psi_{0y}(\pm 1) = \mp s \psi_{0yy}(\pm 1) \quad (13)$$

$$\psi_{1y}(\pm 1) \pm \psi_{0yy}(\pm 1) \cos \alpha(x - t) = \mp s \{ \psi_{1yy}(\pm 1) \pm \psi_{0yyy}(\pm 1) \cos \alpha(x - t) \} \quad (14)$$

$$\psi_{1x}(\pm 1) \pm \psi_{0xy}(\pm 1) \cos \alpha(x - t) = \mp \sin \alpha(x - t) \quad (15)$$

$$\begin{aligned} \psi_{2y}(\pm 1) \pm \psi_{1yy}(\pm 1) \cos \alpha(x - t) + \frac{1}{2} \cos^2 \alpha(x - t) \psi_{0yyy}(\pm 1) \\ = \mp s \{ \psi_{2yy}(\pm 1) \pm \psi_{1yyy}(\pm 1) \cos \alpha(x - t) + \frac{1}{2} \cos^2 \alpha(x - t) \psi_{0yyyy}(\pm 1) \} \end{aligned} \quad (16)$$

$$\psi_{2x}(\pm 1) \pm \psi_{1xy}(\pm 1) \cos \alpha(x - t) + \frac{1}{2} \cos^2 \alpha(x - t) \psi_{0xyy}(\pm 1) = 0 \quad (17)$$

Considering symmetry and a uniform pressure gradient in the x-direction, the solution of the first set of differential equations lead to the following classical Poiseuille flow equation that may be written as

$$\psi_0 = A_0 \left\{ -C_0 y + \sinh \frac{\sqrt{e}y}{\sqrt{k}}, \right\} \quad (18)$$

$$\text{where } C_0 = \frac{\sqrt{e}}{\sqrt{k}} \cosh \frac{\sqrt{e}}{\sqrt{k}} + \frac{se}{k} \sinh \frac{\sqrt{e}}{\sqrt{k}}, \quad A_0 = \frac{kR \left(\frac{\partial p}{\partial x} \right)_0}{C_0}. \quad (19)$$

Let us take the solutions of the differential equations (11) and (12), which satisfy the respective boundary conditions (14), (15) and (16), (17) given by

$$2\psi_1(x, y, t) = \phi_1(y)e^{i\alpha(x-ct)} + \phi_1^*(y)e^{-i\alpha(x-ct)} \quad (20)$$

$$2\psi_2(x, y, t) = \phi_{20}(y) + \phi_{22}(y)e^{2i\alpha(x-ct)} + \phi_{22}^*(y)e^{-2i\alpha(x-ct)}, \quad (21)$$

where the asterisk sign denotes the complex conjugate of the corresponding quantity. We now substitute (20) and (21) into the differential equations (11) and (12) and the boundary conditions (14), (15) and (16), (17). Thus we obtain

$$\left\{ \frac{d^2}{dy^2} - \alpha^2 - \frac{e}{k} + i\alpha e R \left(1 - A_0 \left(-C_0 + \frac{\sqrt{e}}{\sqrt{k}} \cosh \frac{\sqrt{e}y}{\sqrt{k}} \right) \right) \right\} \left\{ \frac{d^2}{dy^2} - \alpha^2 \right\} \phi_1 + \frac{i\alpha R e^{\frac{5}{2}} A_0}{k\sqrt{k}} \cosh \frac{\sqrt{e}y}{\sqrt{k}} \phi_1 = 0 \quad (22)$$

$$\text{with } \phi_1'(\pm 1) + \frac{eA_0}{k} \sinh \frac{\sqrt{e}}{\sqrt{k}} = \mp s\phi_1'' - \frac{se^{\frac{3}{2}}A_0}{k\sqrt{k}} \cosh \frac{\sqrt{e}}{\sqrt{k}}, \quad (23)$$

$$\phi_1(\pm 1) = \pm 1 \quad (24)$$

$$\text{and } \phi_{20}^{iv} - \frac{e}{k}\phi_{20}'' = -\frac{i\alpha e R}{2} (\phi_1\phi_1^{*''} - \phi_1^*\phi_1'')' \quad (25)$$

$$\left\{ \frac{d^2}{dy^2} - 4\alpha^2 - \frac{e}{k} + 2i\alpha e R \left(1 - A_0 \left(-C_0 + \frac{\sqrt{e}}{\sqrt{k}} \cosh \frac{\sqrt{e}y}{\sqrt{k}} \right) \right) \right\} \left\{ \frac{d^2}{dy^2} - 4\alpha^2 \right\} \phi_{22} + \frac{2i\alpha R e^{\frac{5}{2}} A_0}{k\sqrt{k}} \cosh \frac{\sqrt{e}y}{\sqrt{k}} \phi_{22} = \frac{i\alpha e R}{2} (\phi_1'\phi_1'' - \phi_1\phi_1''') \quad (26)$$

along with the conditions

$$\phi_{20}'(\pm 1) \pm \frac{1}{2} (\phi_1''(\pm 1) + \phi_1^{*''}(\pm 1)) + \frac{A_0 e^{\frac{3}{2}}}{2k\sqrt{k}} \cosh \frac{\sqrt{e}}{\sqrt{k}}$$

$$= \mp s \left\{ \phi_{20}''(\pm 1) \pm \frac{1}{2} (\phi_1'''(\pm 1) + \phi_1^{*''' }(\pm 1)) + \frac{A_0 e^2}{2k^2} \sinh \frac{\sqrt{e}}{\sqrt{k}} \right\} \quad (27)$$

$$\begin{aligned} & \phi_{22}'(\pm 1) \pm \frac{1}{2} (\phi_1''(\pm 1) + \phi_1^{*'' }(\pm 1)) + \frac{A_0 e^{\frac{3}{2}}}{4k\sqrt{k}} \cosh \frac{\sqrt{e}}{\sqrt{k}} \\ &= \mp s \left\{ \phi_{22}''(\pm 1) \pm \frac{1}{2} (\phi_1'''(\pm 1) + \phi_1^{*''' }(\pm 1)) + \frac{A_0 e^2}{4k^2} \sinh \frac{\sqrt{e}}{\sqrt{k}} \right\} \end{aligned} \quad (28)$$

$$\phi_{22}(\pm 1) \pm \frac{1}{4} \phi_1'(\pm 1) = 0 \quad (29)$$

In the above-written equations, primes denote derivatives of the function with respect to 'y' and R denotes Reynolds number.

By solving the set of differential equations presented above along with the respective boundary conditions, it is possible to obtain the solution of the problem (up to the second order in ϵ). In the general case, it is difficult to solve the fourth-order differential equations analytically. It is, however, possible to find a closed form solution of the equation for the particular case of pumping of an initially stagnant fluid when there is no imposed pressure gradient, that is $\left(\frac{\partial p}{\partial x}\right)_0 = 0$. In this case, $A_0 = 0$ and the other coefficients are constants. Such a situation occurs in practice, when the fluid is stationary and there is no travelling peristaltic wave. Moreover, the maximum pressure gradient that can be created by a small amplitude is of order ϵ^2 . In the pumping range, the zeroth order mean pressure gradient must disappear. Therefore, the consideration is not much restrictive.

Considering $A_0 = 0$, the solution of equation (22), subject to the boundary conditions (23) and (24) is found as

$$\phi_1(y) = C_{11} \sinh \alpha y + C_{12} \sinh \beta y, \quad (30)$$

in which

$$\begin{aligned} C_{11} &= -\frac{\beta \cosh \beta + s\beta^2 \sinh \beta}{\alpha \cosh \alpha \sinh \beta - \beta \sinh \alpha \cosh \beta + s(\alpha^2 - \beta^2) \sinh \alpha \sinh \beta} \\ C_{12} &= \frac{\alpha \cosh \alpha + s\alpha^2 \sinh \alpha}{\alpha \cosh \alpha \sinh \beta - \beta \sinh \alpha \cosh \beta + s(\alpha^2 - \beta^2) \sinh \alpha \sinh \beta} \end{aligned}$$

$$\text{where } \beta^2 = \alpha^2 + \frac{e}{k} - 2i\alpha e R, \quad (31)$$

when $-d - \eta \leq y \leq d + \eta$.

In order to determine the mean flow, we would need only the term ϕ_{20}' in the expansion of ψ_2 given by (21). Substituting (30) into (25) and integrating w.r.to 'y' we obtain

$$\begin{aligned} \phi_{20}''' - \frac{e}{k} \phi_{20}' &= -\frac{i\alpha R}{2} \left[\left(i\alpha e R - \frac{e}{k} \right) C_{11}^* C_{12} \sinh \alpha y \sinh \beta y + \left(i\alpha e R + \frac{e}{k} \right) C_{11} C_{12}^* \sinh \alpha y \sinh \beta^* y \right. \\ &\quad \left. + 2i\alpha e R C_{12} C_{12}^* \sinh \beta y \sinh \beta^* y \right] + 2C_{20}, \end{aligned} \quad (32)$$

where C_{20} is an arbitrary constant. The equation (32) further leads to

$$\phi'_{20} = f(y) + \frac{\{D - f(1) - sf'(1)\} \cosh \frac{\sqrt{e}y}{\sqrt{k}} - 2C_{20}k}{\cosh \frac{\sqrt{e}}{\sqrt{k}} + \frac{s\sqrt{e}}{\sqrt{k}} \sinh \frac{\sqrt{e}}{\sqrt{k}}} - \frac{2C_{20}k}{e} \left(1 - \frac{\cosh \frac{\sqrt{e}y}{\sqrt{k}}}{\cosh \frac{\sqrt{e}}{\sqrt{k}} + \frac{s\sqrt{e}}{\sqrt{k}} \sinh \frac{\sqrt{e}}{\sqrt{k}}} \right) \quad (33)$$

in which

$$D = \phi'_{20}(\pm 1) \pm s\phi''_{20}(\pm 1) = -\frac{1}{2} \left[\alpha^2 (C_{11} + C_{11}^*) \sinh \alpha + \beta^2 C_{12} \sinh \beta + \beta^{*2} C_{12}^* \sinh \beta^* \right. \\ \left. + s \left\{ \alpha^3 (C_{11} + C_{11}^*) \cosh \alpha + \beta^3 C_{12} \cosh \beta + \beta^{*3} C_{12}^* \sinh \beta^* \right\} \right] \quad (34)$$

$$\text{and } f(y) = -\frac{i\alpha e R}{4} \left[\left(i\alpha e R - \frac{e}{k} \right) C_{11}^* C_{12} \left\{ \frac{\cosh(\alpha + \beta)y}{(\alpha + \beta)^2 - \frac{e}{k}} - \frac{\cosh(\alpha - \beta)y}{(\alpha - \beta)^2 - \frac{e}{k}} \right\} \right. \\ \left. + \left(i\alpha e R + \frac{e}{k} \right) C_{11} C_{12}^* \left\{ \frac{\cosh(\alpha + \beta^*)y}{(\alpha + \beta^*)^2 - \frac{e}{k}} - \frac{\cosh(\alpha - \beta^*)y}{(\alpha - \beta^*)^2 - \frac{e}{k}} \right\} \right. \\ \left. + 2i\alpha e R C_{12} C_{12}^* \left\{ \frac{\cosh(\beta + \beta^*)y}{(\beta + \beta^*)^2 - \frac{e}{k}} - \frac{\cosh(\beta - \beta^*)y}{(\beta - \beta^*)^2 - \frac{e}{k}} \right\} \right] \quad (35)$$

One may note that the constant C_{20} which is proportional to the mean pressure gradient remains arbitrary in the solution. In the equations (1-2), if each term is averaged over an interval of time i.e the period of oscillation, the solution of the present problem can be derived from (8), (18), (20), (21), (30) and (33). The mean pressure gradient may then be expressed as

$$\overline{\frac{\partial p}{\partial x}} = \epsilon^2 \overline{\left(\frac{\partial p}{\partial x} \right)}_2 = \frac{\epsilon^2}{2eR} \phi_{20}''' - \frac{\epsilon^2}{kR} \phi'_{20} + \frac{\epsilon^2}{4} i\alpha (\phi_1 \phi_1^{*''} - \phi_1^* \phi_1'') + O(\epsilon^3) = \frac{\epsilon^2}{eR} C_{20} + O(\epsilon^3) \quad (36)$$

As a natural consequence of (36), we can write

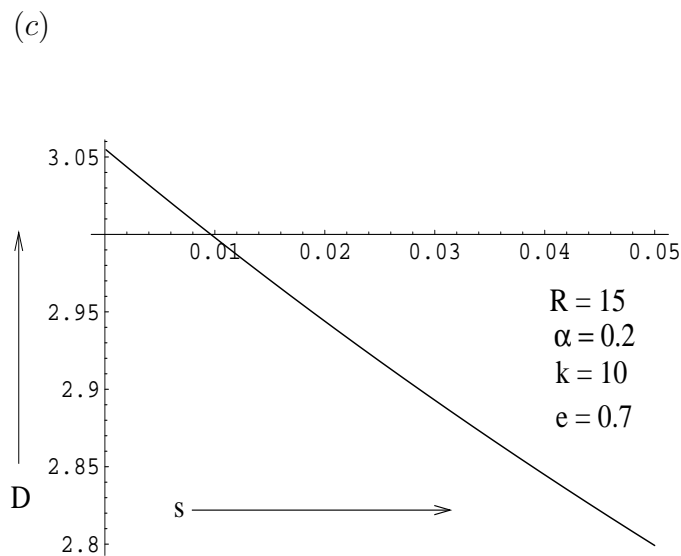
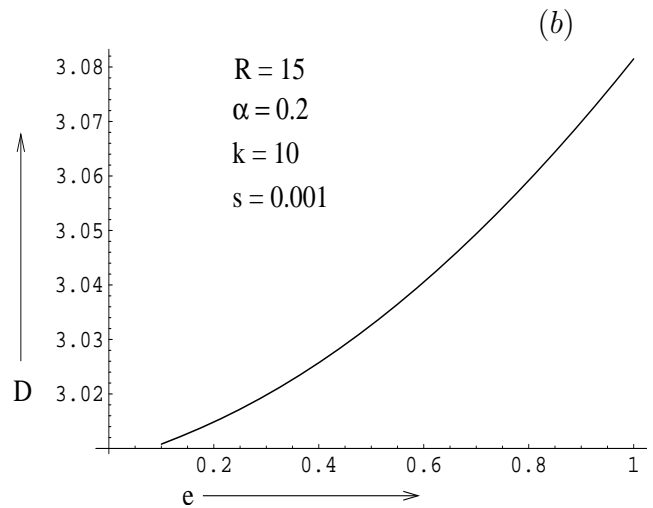
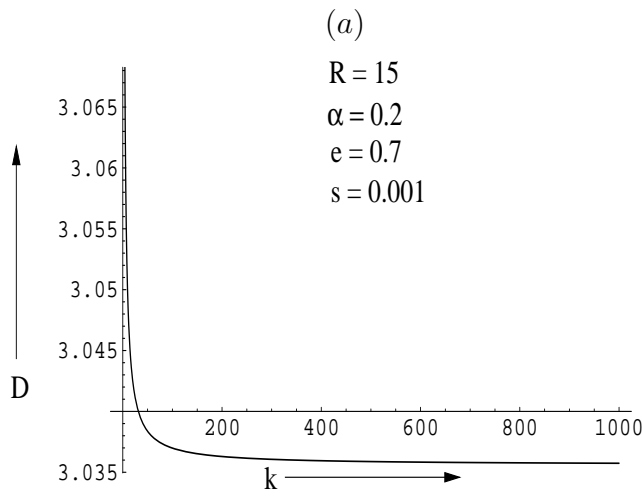
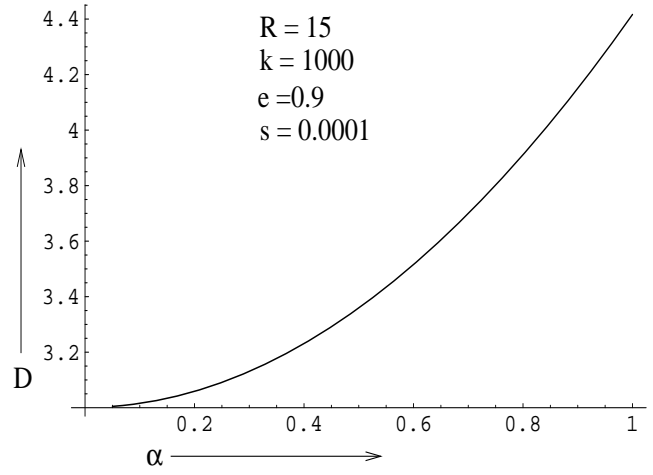
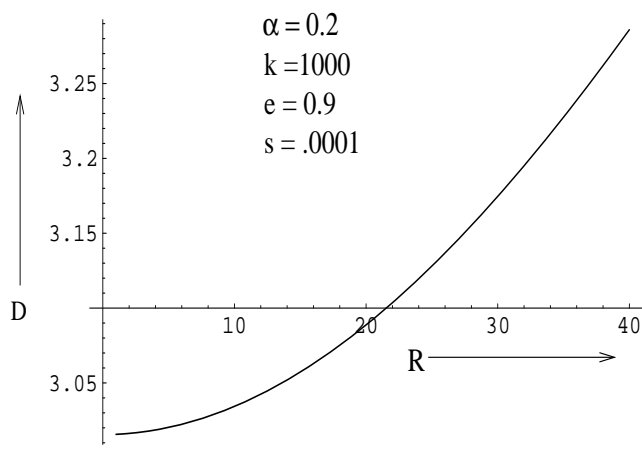
$$\overline{\left(\frac{\partial p}{\partial x} \right)}_2 = \frac{C_{20}}{eR} \quad (37)$$

It is now clear that C_{20} is proportional to the time averaged pressure gradient arising out of the peristaltic motion of the fluid. Its value can be determined by employing the conditions for a given physiological problem. Noting that $\overline{\left(\frac{\partial p}{\partial x} \right)}_2$ is independent of the y-coordinate, the expression for the mean velocity in the axial direction can be put in the form

$$\bar{u} = \frac{\epsilon^2}{2} \phi'_{20} = \frac{\epsilon^2}{2} \left[f(y) + \frac{(D - f(1) - sf'(1)) \cosh \frac{\sqrt{e}y}{\sqrt{k}} - 2C_{20}k}{\cosh \frac{\sqrt{e}}{\sqrt{k}} + \frac{s\sqrt{e}}{\sqrt{k}} \sinh \frac{\sqrt{e}}{\sqrt{k}}} - \frac{2C_{20}k}{e} \left(1 - \frac{\cosh \frac{\sqrt{e}y}{\sqrt{k}}}{\cosh \frac{\sqrt{e}}{\sqrt{k}} + \frac{s\sqrt{e}}{\sqrt{k}} \sinh \frac{\sqrt{e}}{\sqrt{k}}} \right) \right] \quad (38)$$

Using (36), we can alternatively write

$$\bar{u} = \frac{\epsilon^2}{2} \left[f(y) + \frac{(D - f(1) - sf'(1)) \cosh \frac{\sqrt{e}y}{\sqrt{k}}}{\cosh \frac{\sqrt{e}}{\sqrt{k}} + \frac{s\sqrt{e}}{\sqrt{k}} \sinh \frac{\sqrt{e}}{\sqrt{k}}} - 2kR \overline{\left(\frac{\partial p}{\partial x} \right)}_2 \left(1 - \frac{\cosh \frac{\sqrt{e}y}{\sqrt{k}}}{\cosh \frac{\sqrt{e}}{\sqrt{k}} + \frac{s\sqrt{e}}{\sqrt{k}} \sinh \frac{\sqrt{e}}{\sqrt{k}}} \right) \right] \quad (39)$$



(e)

Fig. 2: Variation of D with R , α , Darcy number, porosity and slip parameter

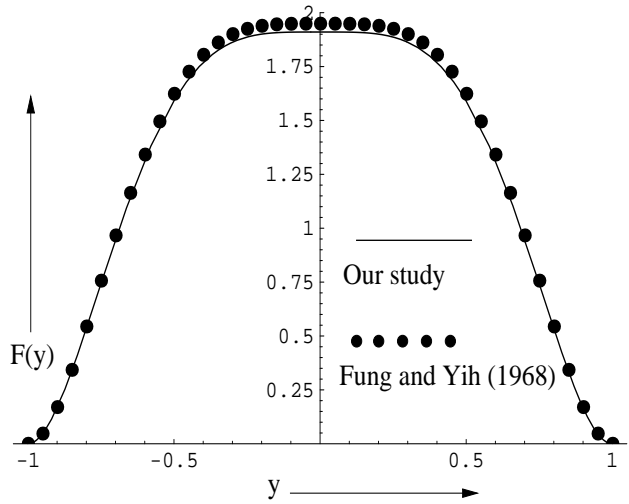


Fig.3

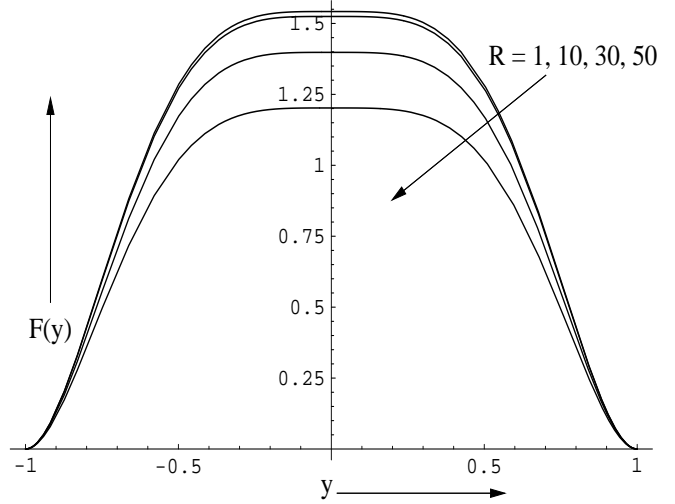


Fig.4

Fig. 3-4: Mean velocity perturbation function $F(y)$, Fig3: Comparison of our result with Fung and Yih [2] for $R=1$, $\alpha = 0.4$, $k=10000$, $e=0.99$, $s=0.00001$; Fig4: Distribution of $F(y)$ for different values of R with $\alpha = 0.25$, $k=1000$, $e=0.9$, $s=0.00001$

For a problem such as the one under our present considerations, it is worthwhile to determine the critical reflux condition. This is the condition that determines the location of the point on the central line ($y=0$) at which the mean velocity $\bar{u}(y)$ vanishes. Using (39), the critical reflux condition for the problem is derived in the form

$$\left(\frac{\partial p}{\partial x}\right)_{2 \text{ critical reflux}} = \frac{1}{2kR} \left[\frac{f(0) \left(\cosh \frac{\sqrt{e}}{\sqrt{k}} + \frac{\sqrt{e}}{\sqrt{k}} \sinh \frac{\sqrt{e}}{\sqrt{k}} \right) + D - f(1) - s f'(1)}{\cosh \frac{\sqrt{e}}{\sqrt{k}} + \frac{s\sqrt{e}}{\sqrt{k}} \sinh \frac{\sqrt{e}}{\sqrt{k}} - 1} \right] \quad (40)$$

Use of this critical value enables us to study the mean velocity distribution $\bar{u}(y)$ at the critical reflux condition.

4 Numerical Results and Discussion

In the last section, we have presented the analytical expressions of the velocity, time-averaged velocity and critical pressure for reflux for the problem under consideration. In this section, we intend to investigate the problem and present the computational results for the said quantities graphically. Computation has been performed by making use of available experimental and theoretical data of bile. The different parameters involved in our forgoing theoretical analysis

are Reynolds number R , pressure gradient, porosity parameter e , Darcy number k , slip parameter, amplitude ratio and wave number. Computation of the time-averaged velocity and critical pressure for reflux has been carried out by extensive use of the software Mathematica.

4.1 Average Velocity in Bile Transport

Numerical computation based on equation (39) reveals that the averaged axial velocity of bile (if treated as a Newtonian fluid) flowing in a porous medium is dominated by the constant

$$\frac{D}{\cosh \frac{\sqrt{e}}{\sqrt{k}} + \frac{s\sqrt{e}}{\sqrt{k}} \sinh \frac{\sqrt{e}}{\sqrt{k}}} \text{ and the parabolic distribution term } 2kR \overline{\left(\frac{\partial p}{\partial x}\right)}_2 \left(1 - \frac{\cosh \frac{\sqrt{e}y}{\sqrt{k}}}{\cosh \frac{\sqrt{e}}{\sqrt{k}} + \frac{s\sqrt{e}}{\sqrt{k}} \sinh \frac{\sqrt{e}}{\sqrt{k}}}\right)$$

In addition to these two terms, there is an expression

$$G(y) = f(y) - \frac{(f(1) + sf'(1)) \cosh \frac{\sqrt{e}y}{\sqrt{k}}}{\cosh \frac{\sqrt{e}}{\sqrt{k}} + \frac{s\sqrt{e}}{\sqrt{k}} \sinh \frac{\sqrt{e}}{\sqrt{k}}} \quad (41)$$

that represents the perturbation of the velocity across the channel. Its distribution controls the direction of peristaltic mean flow across the cross-section of the bile duct. It is evident from (33) and (31) that the constant D that gives the value of ϕ'_{20} at the boundary depends on Reynolds number, porosity, Darcy number, slip parameter and wave number. It arises from the expression of the radial component of the first-order axial velocity gradient and is connected with the offset boundary condition (27). It may be mentioned here that the no-slip/velocity-slip applies to the wavy wall and not to the mean position of the wall. Figs. 2(a-e) give the variation of D with the parameters Reynolds number, porosity, Darcy number, wave number and velocity-slip.

Furthermore, the parabolic mean velocity distribution term $-2kC_{20} \left(1 - \frac{\cosh \frac{\sqrt{e}y}{\sqrt{k}}}{\cosh \frac{\sqrt{e}}{\sqrt{k}} + \frac{s\sqrt{e}}{\sqrt{k}} \sinh \frac{\sqrt{e}}{\sqrt{k}}}\right)$ arises out of the time – averaged second order pressure gradient $\overline{\left(\frac{\partial p}{\partial x}\right)}_2 = \frac{C_{20}}{eR}$.

We define $F(y) = -\frac{200}{\alpha^2 R^2} G(y)$, $G(y)$ being given by (41). Fig.3 depicts the nature of the function $F(y)$. With an aim to validate our results, we have presented in the same figure the results reported by Fung and Yih [2] who did not account for the Darcy number, porosity and velocity-slip. It is needless to mention that the results presented in this figure on the basis of our study correspond to the case when Darcy number, porosity and velocity-slip are neglected (for the

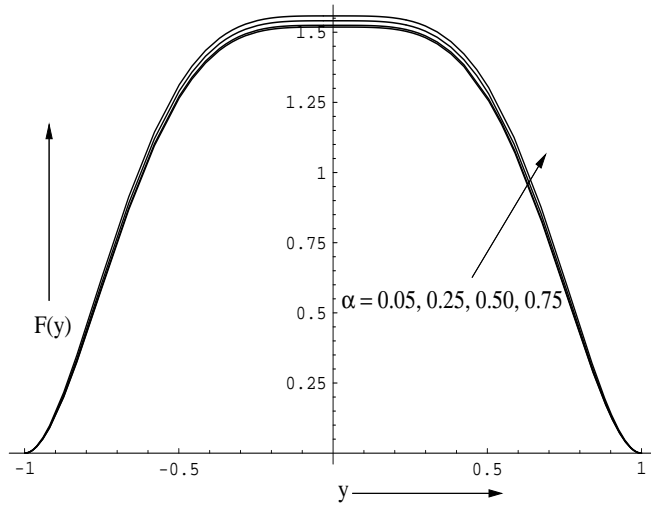


Fig.5

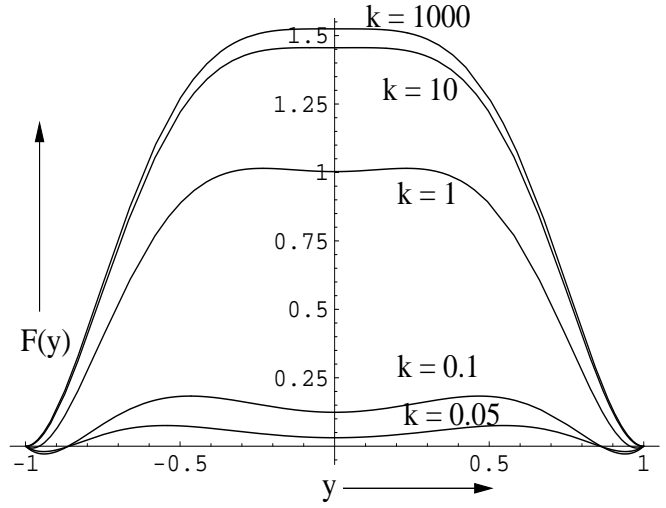


Fig.6

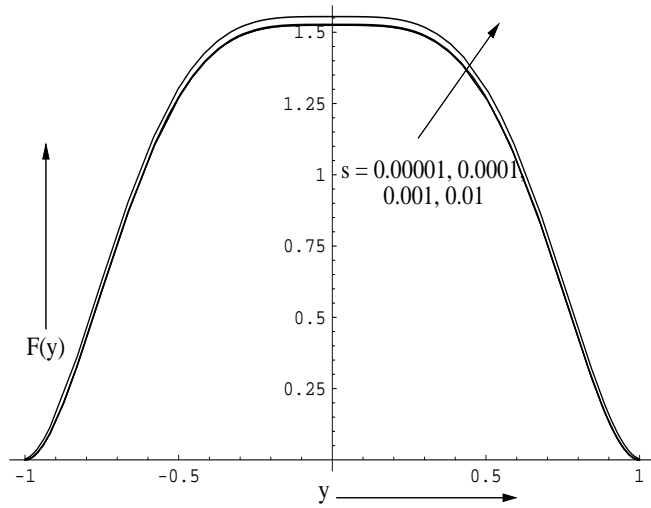


Fig.7

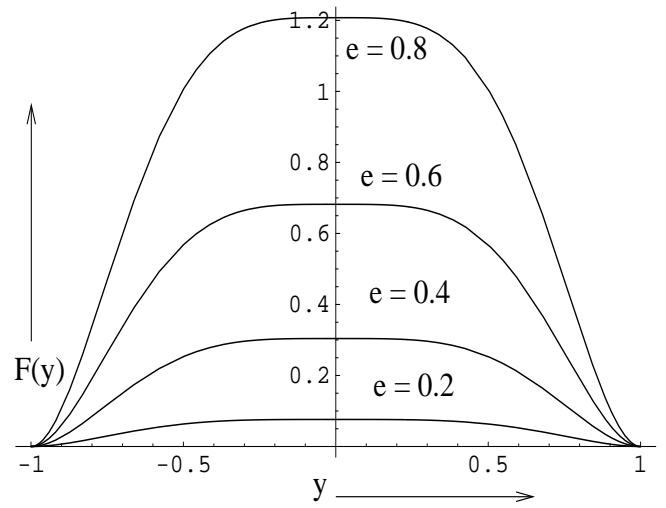


Fig.8

Figs. 5-8: Mean velocity perturbation function $F(y)$ (Fig5.) for different values of α with $R=10$, $k=1000$, $e=0.9$, $s=0.00001$; (Fig6.) for different values of k with $R=10$, $\alpha=0.25$, $e=0.9$, $s=0.00001$; (Fig7.) for different values of e with $R=10$, $\alpha=0.25$, $k=1000$, $s=0.00001$; (Fig8.) for different values of s with $R=10$, $\alpha=0.25$, $e=0.9$, $k=1000$

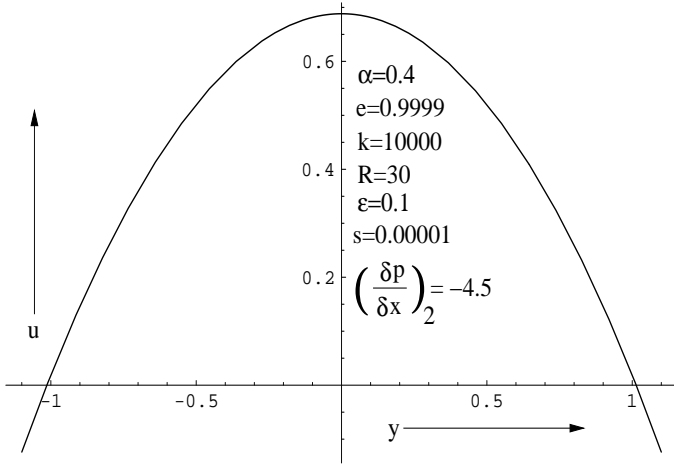


Fig.9.1

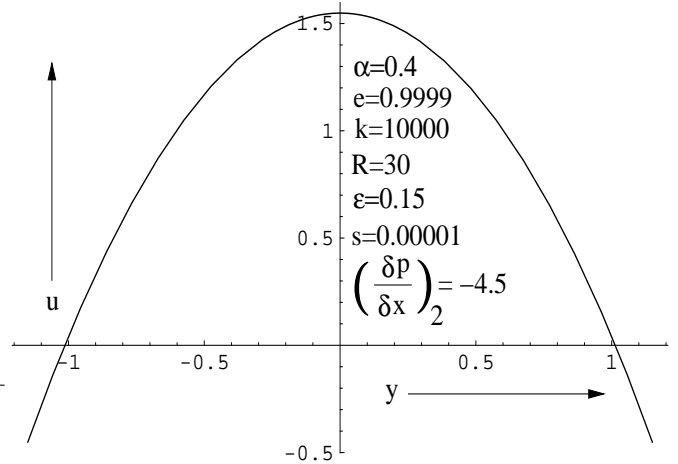


Fig.9.2

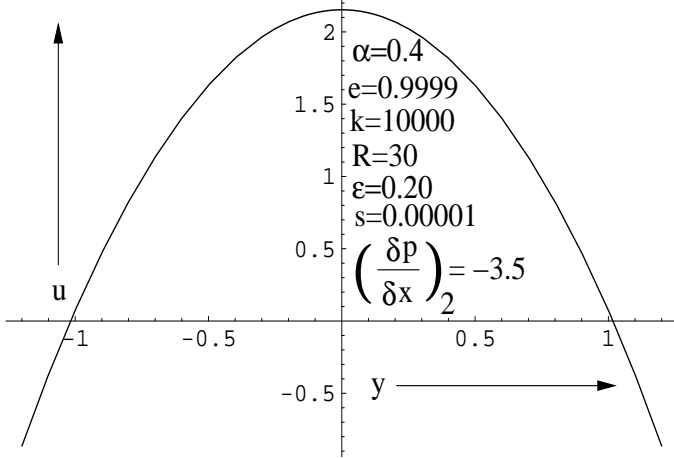


Fig.9.3

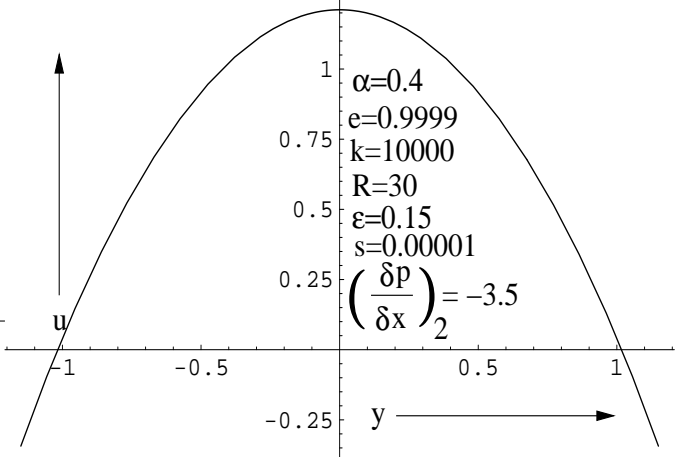


Fig.9.4

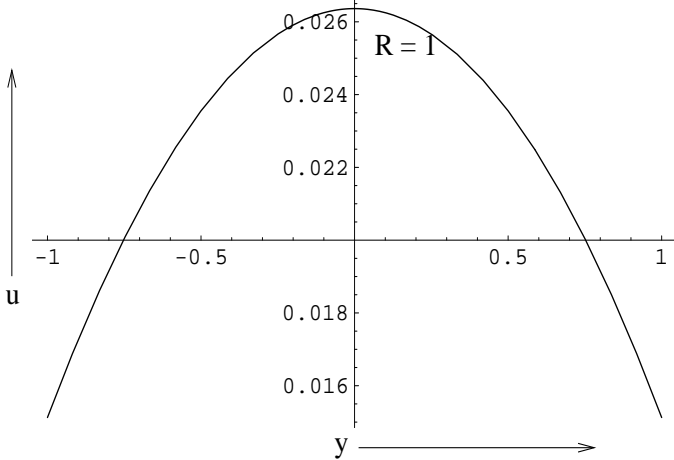


Fig.9.5

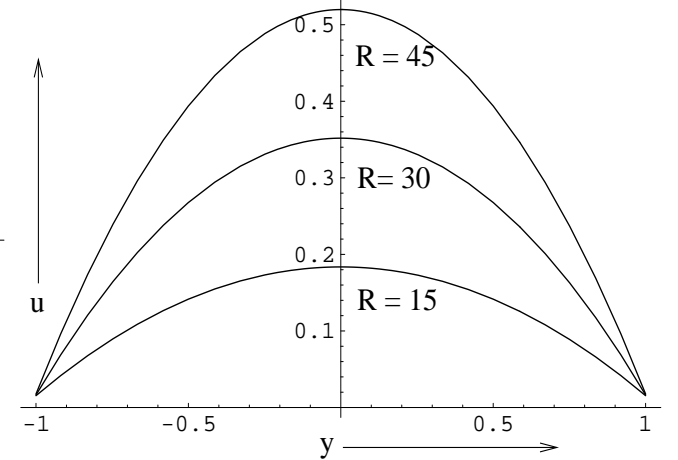


Fig.9.6

Figs. 9: Time-averaged mean axial velocity profiles for different values of R when $\alpha=0.25$, $e=0.9$, $\epsilon=0.1$, $\left(\frac{\partial p}{\partial x}\right)_2 = -2.5$, $k=1000$, $s=0.0001$

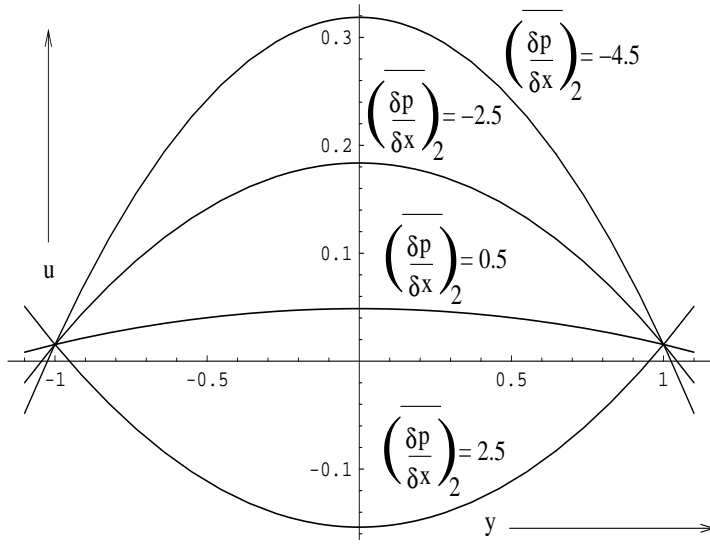


Fig.10.1

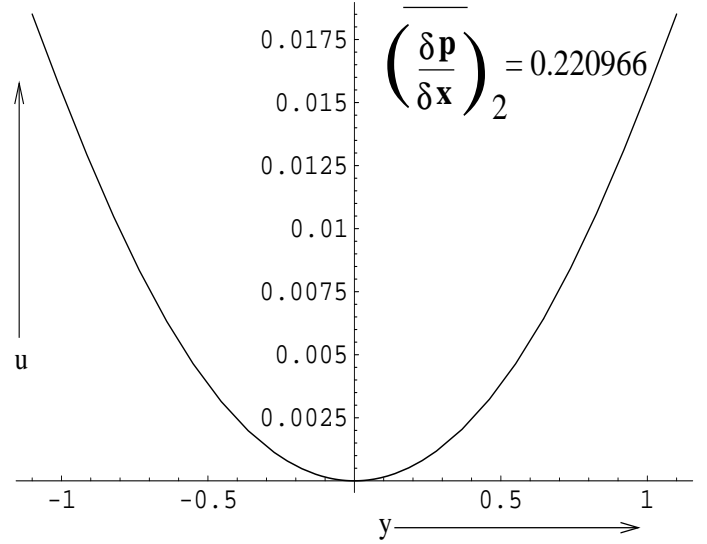


Fig.10.2

Figs. 10: Time-averaged mean axial velocity profiles for different values of $\left(\frac{\partial p}{\partial x}\right)_2$ when $R=15$, $\alpha=0.25$, $e=0.9$, $\epsilon=0.1$, $k=1000$, $s=0.0001$

sake of meaningful comparison/validation). It may be noted that the results of both the studies have a very close resemblance. In Fig. 4 we have presented the nature of variation of $F(y)$ for different values of the Reynolds number for a particular set of values of α , k , e and s . This figure shows that $F(y)$ decreases as the Reynolds number R increases. This observation is in conformity to that reported in [2]. It may be noted from Figs. 5 and 7 that in the ranges of values for α (wave number) and s (slip parameter) considered here, the change in the function $F(y)$ is not very much significant.

Figs. 6 and 8 reveal that with the increase in the Darcy number k and the porosity parameter e , the perturbation term $F(y)$ increases. The results correspond to the case of bile containing stones. Figs. 9-15 illustrate the individual contribution of Reynolds number, pressure gradient, amplitude ratio, Darcy number, the porosity parameter, slip parameter and wave number on the time-averaged mean axial velocity profile. It is found that the mean axial velocity increases with an increase in Reynolds number (See Figs. 9). It is important to note (cf. Figs. 10) that reflux occurs in the central region when pressure gradient attains a certain critical value 0.220966. Fig. 11 illustrates that the bile flow is strongly dependent on the amplitude ratio of the wave. It reveals that bile velocity is enhanced with the increase in amplitude ratio and that flow reversal takes place near the boundary for higher values of the amplitude ratio. These results are in conformity (cf. Figs. 9.1-4) to those of an experimental study conducted by Sugita et al.

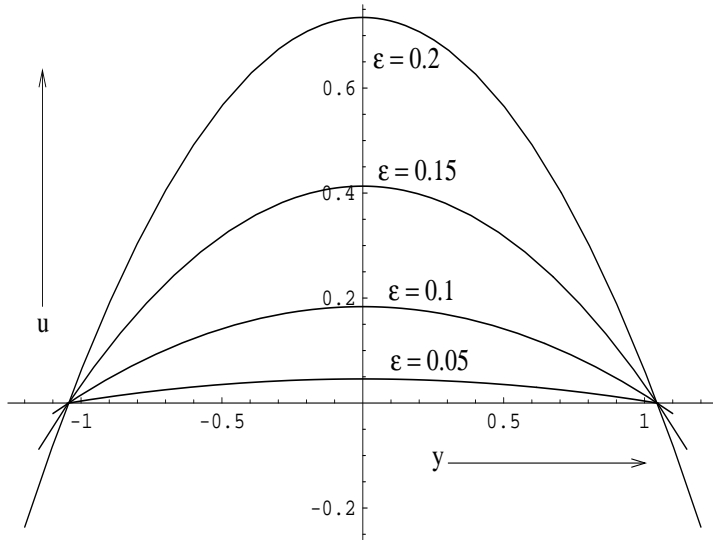


Fig.11

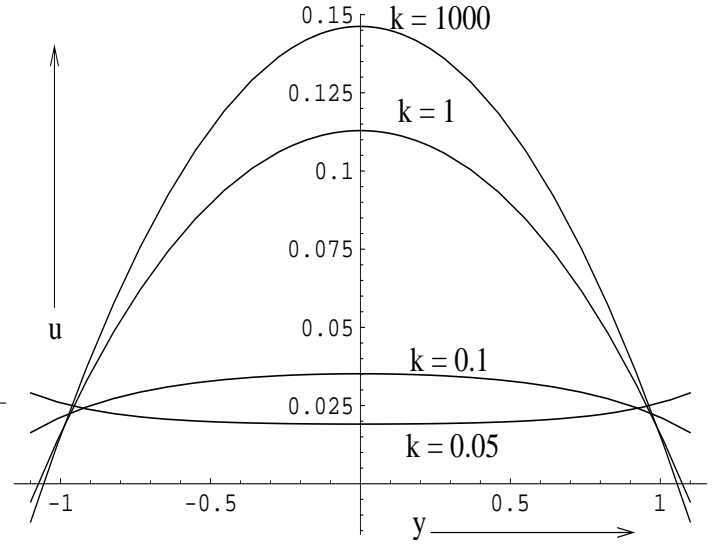
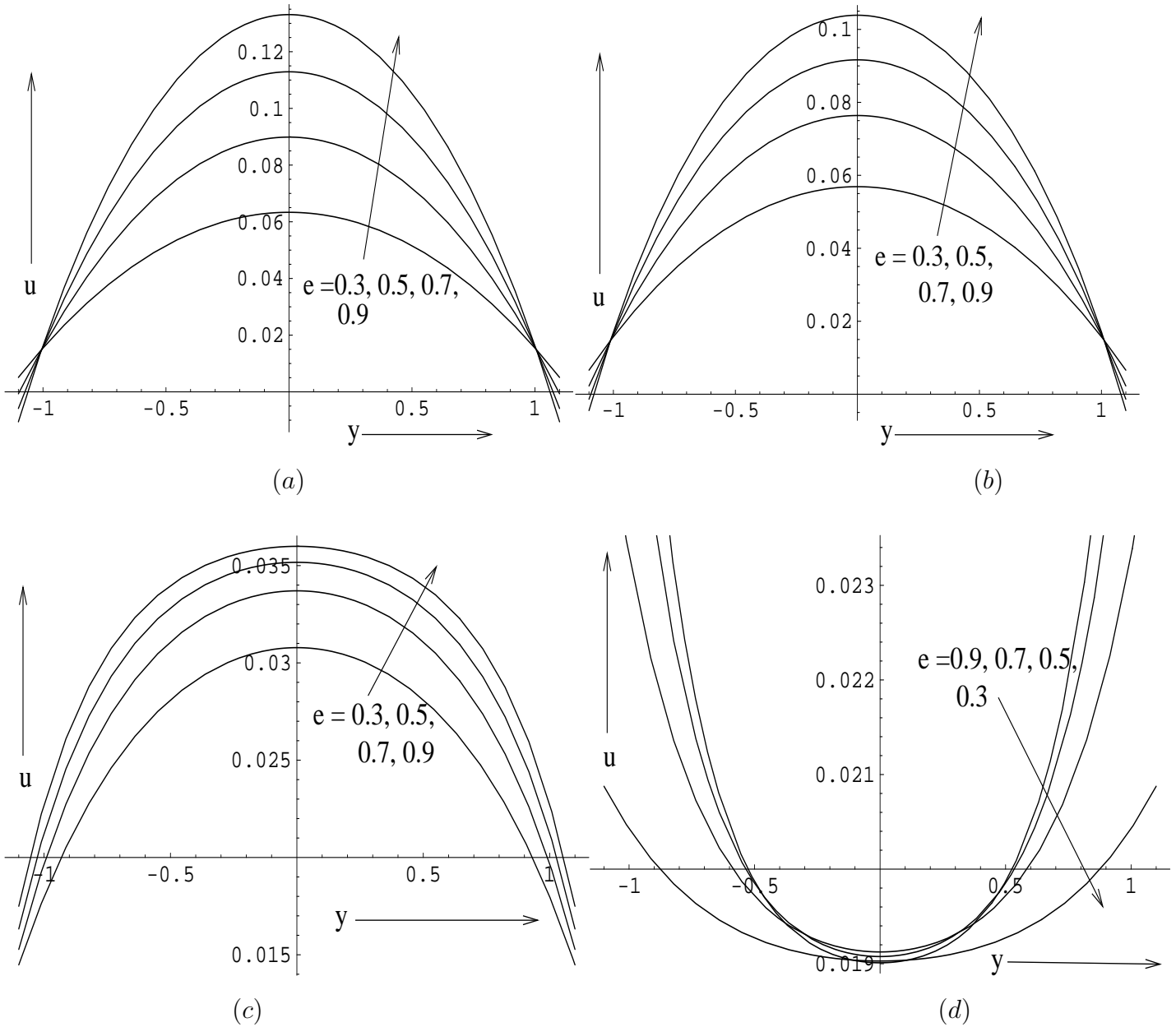


Fig.12

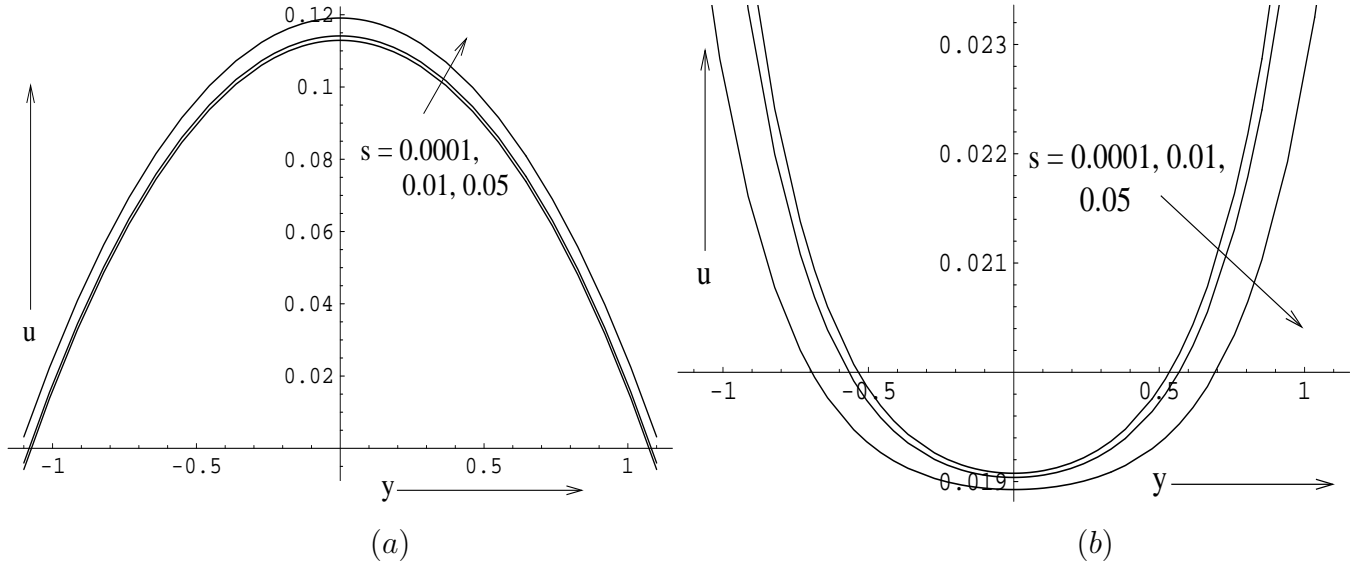
Figs. 11-12: Time averaged mean axial velocity profiles, Fig. 11: for different values of ϵ when $R=15$, $\alpha=0.25$, $e=0.9$, $\left(\frac{\partial p}{\partial x}\right)_2 = -2.5$, $k=1000$, $s=0.0001$; Fig. 12: for different values of k when $R=15$, $\left(\frac{\partial p}{\partial x}\right)_2 = -2.5$, $\alpha=0.25$, $e=0.9$, $\epsilon=0.1$, $s=0.0001$

[35]. They investigated pseudolesion of the bile duct caused by flow effect and observed that at 1.0mm/sec. intervals flow speed of bile ranges between 1.0 and 20 mm/sec. approximately. It may be noted from Fig. 12 that although in the central region of the channel, the velocity reduces with the decrease in the Darcy number, the velocity profiles are quite different from the familiar Poiseuille profile. This shows that the bile velocity decreases as the number of stones increases.

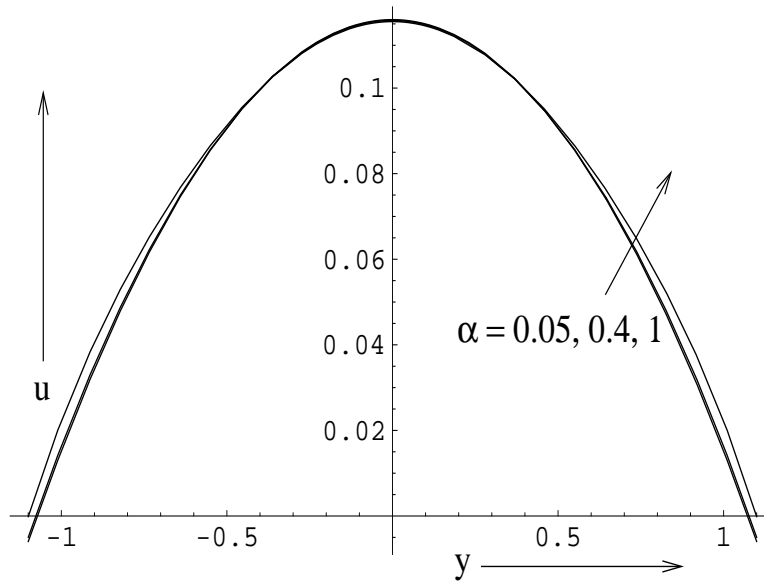
Fig. 13 depicts the variation of the velocity profiles with the porosity parameter e for fixed values of Reynolds number, pressure gradient, slip parameter, amplitude ratio and wave number. The velocity is found to increase, as the porosity parameter increases in the case when the Darcy number exceeds the value 0.05, though its parabolic nature changes for small Darcy number. Thus in the situation as the number of stones decreases, the bile velocity gradually increases and in the absence of any stone, the bile velocity will be the greatest. The occurrence of a reverse trend is observed when the Darcy number equals 0.05. Fig. 14 shows that velocity-slip has a strong influence on the axial velocity in the porous case. From Fig. 15, it is observed that wave number affects the axial velocity more prominently in the vicinity of the boundary.



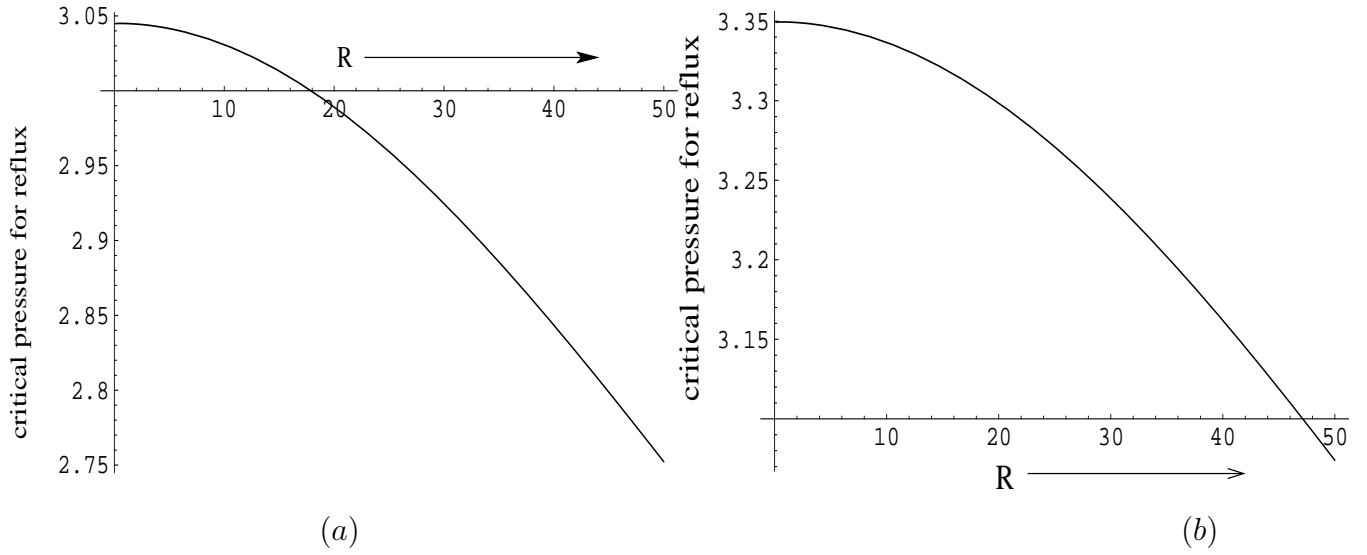
Figs. 13: Time averaged mean axial velocity profiles for different values of e when $R=15$, $\epsilon=0.1$, $\alpha=0.25$, $\overline{\left(\frac{\partial p}{\partial x}\right)}_2 = -2.5$, $s=0.0001$ (a) $k=1$; (b) $k=0.5$; (c) $k=0.1$; (d) $k=0.05$



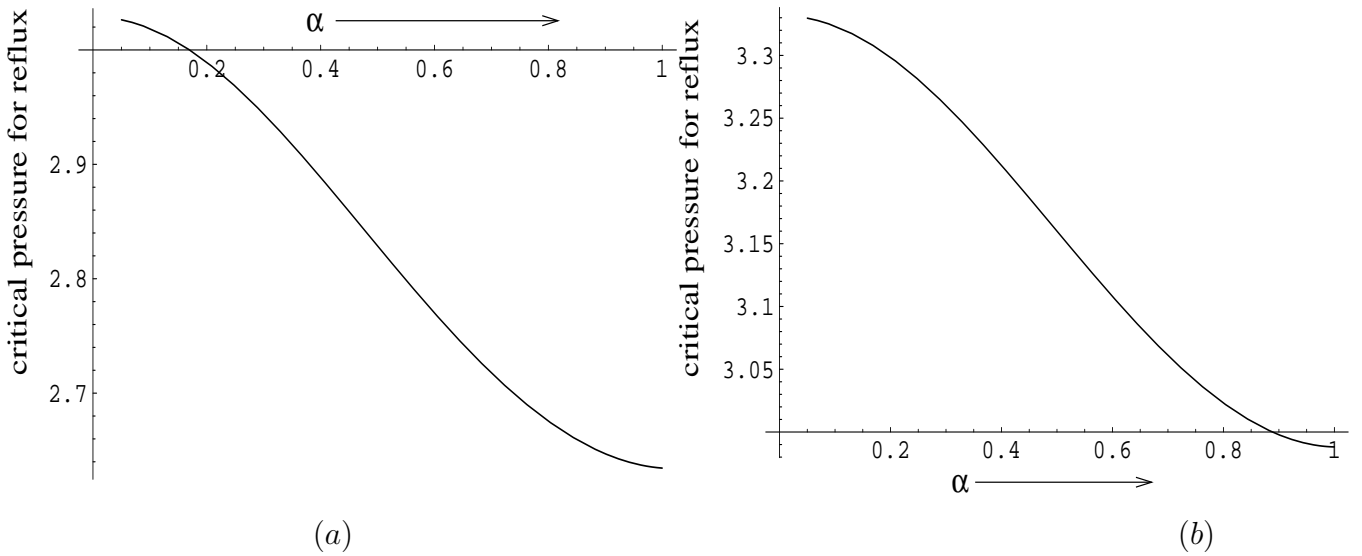
Figs.: 14: Time averaged mean axial velocity profiles for different values of s when $R=15$, $\epsilon=0.1$, $\alpha=0.25$, $\left(\frac{\partial p}{\partial x}\right)_2 = -2.5$, $e=0.7$ (a) $k=1$; (b) $k=0.05$



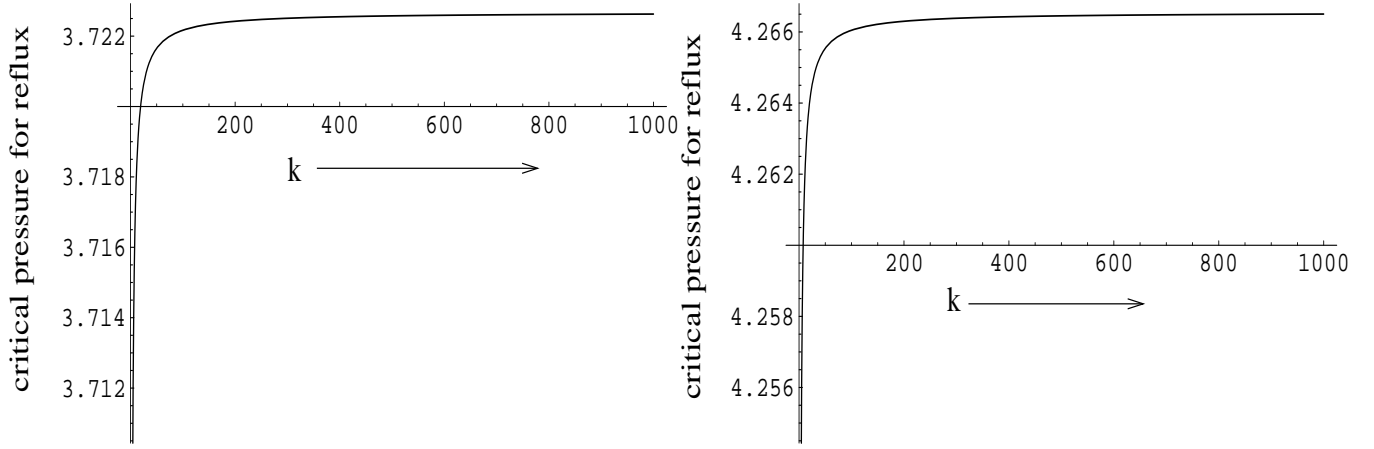
Figs. 15: Time averaged mean axial velocity profiles for different values of α when $R=15$, $\epsilon=0.1$, $\left(\frac{\partial p}{\partial x}\right)_2 = -2.5$, $e=0.7$, $k=100$, $s=.001$



Figs. 16: Effect of the Reynolds number on $\overline{\left(\frac{\partial p}{\partial x}\right)_{2critical\ reflux}}$ when $\alpha=0.2$, $k=1000$, $s=0.0001$
 (a) $e=0.99$; (b) $e=0.9$



Figs. 17: Effect of α on $\overline{\left(\frac{\partial p}{\partial x}\right)_{2critical\ reflux}}$ $R=20$, $k=1000$, $s=0.0001$ (a) $e=0.99$; (b) $e=0.9$



(a) (b)

Figs. 18: Effect of k on $\overline{\left(\frac{\partial p}{\partial x}\right)}_{2critical\ reflux}$ $R=20$, $\alpha=0.2$, $s=0.0001$ (a) $e=0.8$; (b) $e=0.7$

4.2 Critical Pressure for Reflux

It is known that bacteria and some other materials sometimes move from the bladder to the kidney or from one kidney to the other in the direction opposite to the direction of urine flow. This phenomenon is referred to as 'ureteral reflux' by physiologists. Severity of diseases such as tuberculosis, interstitial cystitis, duct stone etc. is often enhanced due to this reflux. It may also happen that due to reflux, from the common bile duct, bile flows into the gallbladder and is stored there. Results for the critical pressure for reflux $\overline{\left(\frac{\partial p}{\partial x}\right)}_{2\ critical\ reflux}$ computed from equation (40) are displayed in Figs. 16-20. Results presented in Figs. 16 match with those of Fung and Yih [2]. This figure illustrates that the said critical reflux decreases as the Reynolds number increases. It is observed from Figs. 17-19 that the critical pressure reduces with an increase in wave number, whereas it first increases with the increase in Darcy number and subsequently maintains nearly a constant value. It is also worthwhile to observe that the porosity parameter significantly affects the magnitude of the critical pressure. From Fig. 18, it can be conjectured that when the number of stones in the bile is very high, reflux occurs when the critical pressure is relatively small. The effect of slip parameter on the critical reflux is revealed in Figs. 20.

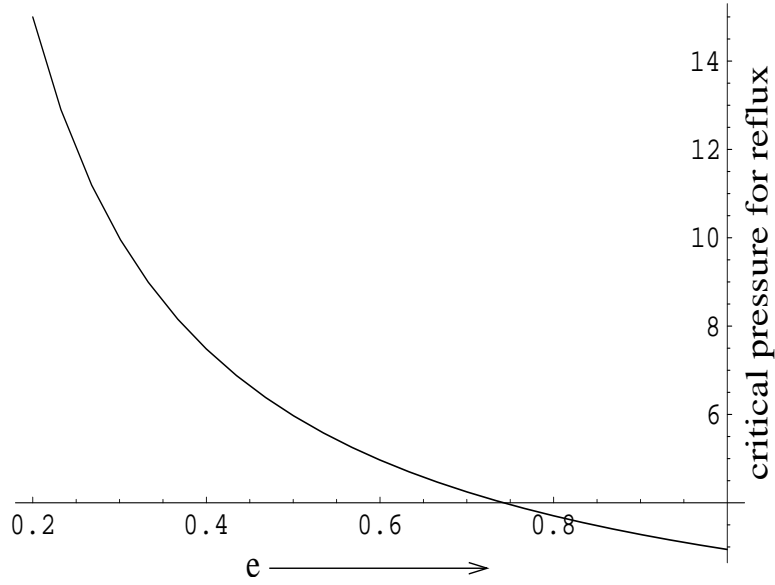


(Fig. 19)

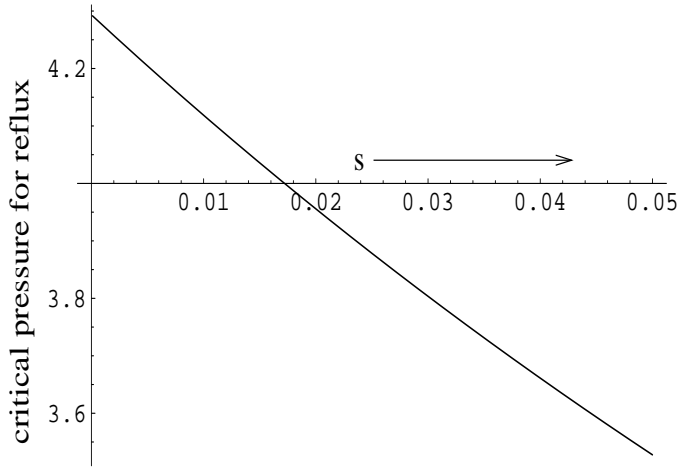
Figs. 19: Effect of e on $\overline{\left(\frac{\partial p}{\partial x}\right)}_{2critical\ reflux}$ $R=20, \alpha=0.2, k=10, s=0.001$

5 Summary and Conclusion

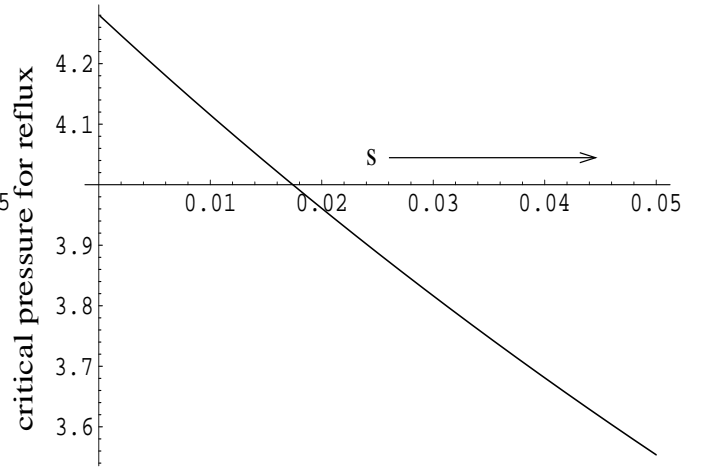
The peristaltic transport of a fluid has been investigated here. The flow is considered to take place in a porous channel. The study pertains more particularly to a situation where the Reynolds number is low and the curvature of the channel is quite small. The specific problem has got relevance to the physiological problem of flow of bile in the common bile duct (cf. [3, 25, 26, 27, 35, 36, 37, 38, 39]). As mentioned in Section 1, bile flow takes place peristaltically and the common bile duct is porous. The results presented are applicable to bile flow in the pathological state, where stones are formed in the bile. Evidence of slip velocity in bile flow has also been mentioned in Section 1. An attempt has been made to investigate to some important bio-fluid dynamical phenomena associated with peristaltic transport.

Quantitative estimates have been presented for the axial velocity and critical pressure for reflux as a function of Reynolds number, pressure gradient, porosity parameter, Darcy number, slip parameter, amplitude ratio as well as wave number. The results and observations are found to be in good agreement with those reported in [2, 33, 34, 35].

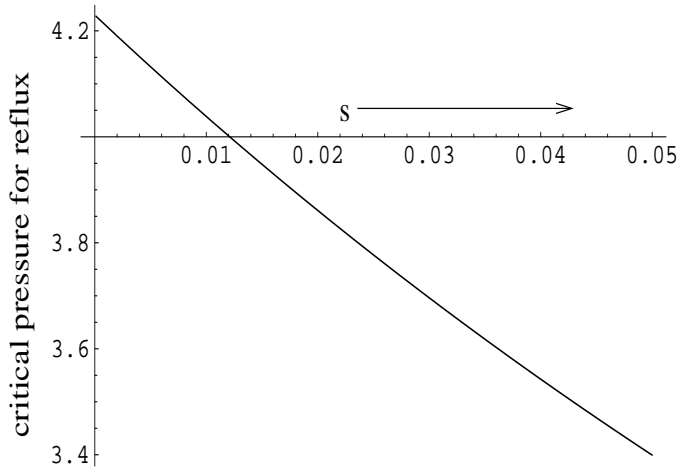
From the observations of this study, it reveals that the velocity profile strongly depends on several parameters, viz. the mean pressure gradient, porosity, Darcy number as well as amplitude



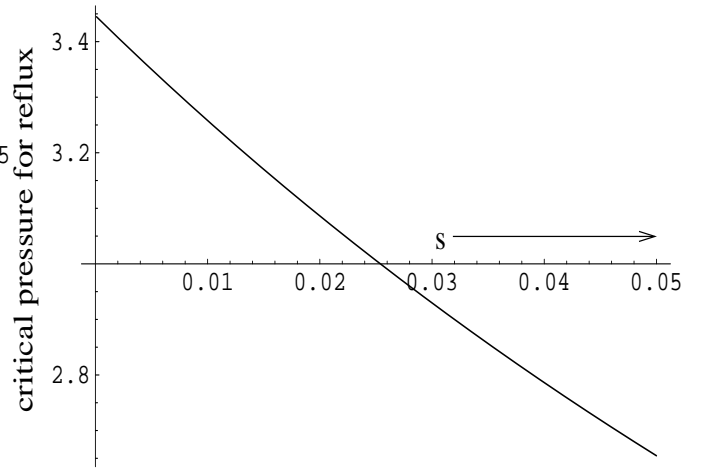
(a)



(b)



(c)



(d)

Figs. 20: Effect of s on $\overline{\left(\frac{\partial p}{\partial x}\right)_{2critical\ reflux}}$ $e=0.7$, $\alpha=0.2$, (a) $R=10$, $k=10$; (b) $R=15$, $k=10$; (c) $R=15$, $k=1$; (d) $R=15$, $k=0.1$

ratio. The study further indicates that the reflux will occur if pressure gradient attains a certain critical value.

The present theoretical investigation motivated towards the peristaltic transport of bile in the bile duct in the presence of stones can serve as a model that bears the potential to enrich our understanding of the related physiology of the problem. The important conjectures that can be made out of the study are as follows :

- (i) Bile velocity decreases as the stones increases.
- (ii) When bile contains a very large number of stones, reflux occurs when the critical pressure is quite small.

Acknowledgment: *The authors wish to express their deep sense of gratitude to all the reviewers for their kind appreciation and the estimated comments on the work. One of the authors (Somnath Maiti) is thankful to the Council of Scientific and Industrial Research (CSIR), New Delhi for their financial support towards this study.*

References

- [1] Shapiro, A.H., Jaffrin, M.Y. and Weinberg, S.L., “Peristaltic pumping with long wavelength at low Reynolds number”, J. Fluid Mech. 37 (1969), 799-825.
- [2] Fung Y.C. and Yih C.S., “Peristaltic Transport”, J. Appl. Mech. 35 (1968), 669-75.
- [3] Daniel, E. E.; Tomita, T and Watanabe, M., “Sphincters: Normal Function - Changes in Disease”, chapt. 13 (1992), Oddi: Pathophysiology (by J. Toouli and G.T.P.Saccone), page no.201.
- [4] Usha, S. and Rao, A. R., “Effect of curvature and inertia on the peristaltic transport in a two fluid system”, Int. J. Engng. Sci., 38 (2000), 1355-75.
- [5] Mishra, M. and Rao, A.R. “Peristaltic transport of a Newtonian fluid in an asymmetric channel ”, ZAMP. 54 (2003), 532-50.
- [6] Mishra, M. and Rao, A.R., “Peristaltic transport of a power law fluid in a porous tube”, J.Non-Newtonian Fluid Mech. 121 (2004), 163-74.
- [7] Misra, J.C. and Pandey, S.K., “Peristaltic transport of a non-Newtonian fluid with a peripheral layer”, Int. J. Engng. Sci. 37 (1999), 1841-58.
- [8] Misra, J.C. and Pandey, S.K., “Peristaltic flow of a multi layered power-law fluid through a cylindrical tube”, Int. J. Engng. Sci. 39 (2001), 387-402.

- [9] Misra, J.C. and Pandey, S.K., “Peristaltic transport of a particle-fluid suspension in a cylindrical tube”, *Comput. Math. Appl.* 28 (1994), 131-45.
- [10] Misra, J.C. and Pandey, S.K., “Peristaltic transport of blood in small vessels: study of a mathematical model”, *Comput. Math. Appl.*,43 (2002), 1183-93.
- [11] Misra, J.C and Pandey, S.K, “Peristaltic transport in a tapered tube”, *Math. Compu. Model.*, 22(8) (1995), 137-151
- [12] Misra, J.C., Maiti S., Shit G.C, “Peristaltic Transport of a Physiological Fluid in an Asymmetric Porous Channel in the Presence of an External Magnetic Field”, *J. Mech. Med. Biol.*, 8(4) (2008), 507-525.
- [13] Eytan, O., Jaffa, A.J. and Elad, D., “Peristaltic flow in a tapered channel: application to embryo transport within the uterine cavity”, *Med. Engng. Phy.* 23 (2001), 473-82.
- [14] Taylor, G.I., “Analysis of the swimming of microscopic organisms”, *Proc. Roy. Soc. Lond. A* 209 (1951), 447-61.
- [15] Pozrikidis, C.” A study of Peristaltic flow”, *J.Fluid Mech.* 180 (1987), 515-27.
- [16] Carew,E.O and Pedley, T.J., “An active membrane model for peristaltic pumping: Part I-Periodic activation waves in an infinite tube”, *J. Biomech. Eng.* 119 (1997), 66-76.
- [17] Antanovskii, L.K and Ramkissoon, H., “Long-wave peristaltic transport of a compressible viscous fluid in a finite pipe subject to a time-dependent pressure drop”, *Fluid Dynamics Research.* 19 (1997), 115-123.
- [18] Vries, K.D., Lyons, E.A., Ballard, J., Levi, C.S. and Lindsay, D.J., “Contractions of the inner third of myometrium”, *Am.J.Obstetries Gynecol.* 162 (1990), 679-82.
- [19] Keener, J.R. and Sneyd, J., “Mathematical Physiology”, Springer, 1998.
- [20] Berrgel, D.H., “Cardiovascular Fluid Dynamics”, Academic Press, London, 1972.
- [21] Li, A., Nesterov, N.I. Malikova,S.N. and Kiiatkin, V.A.“The use of an impulse magnetic field in the combined of patients with stone fragments in the upper urinary tract”, *Vopr kurortol Fizioter Lech Fiz Kult* 3 (1994), 22-24.
- [22] Torsoli, A. and Ramorino, M. L., “Motility of the Biliary Tract”, *Rendiconti Romani di Gastro Enterologica* 2 (1970), 67-80.
- [23] Everhartet J.E, Khare M, Hill M and Maurer K.R., “Prevalence and ethnic differences in gallbladder disease in the United States”, *Gastroenterology* 117 (1999), 632-9.
- [24] Khuroo M.S, Mahajan R, Zargar S.A, Javid G and Sapru S., “Prevalence of biliary tract disease in India: A sonographic study in adult population in Kashmir”, *Gut* 30 (1989), 201-5.

- [25] Bennion L.J and Grundy S.M., “Risk factors for development of cholelithiasis in man”, *N Engl J Med* 299 (1978), 1221-7.
- [26] Maclure K.M, Hayes K.C, Colditz G.A, Stampfer M.J, Speizer F.E and Willet W.C., “Weight, diet and the risk of symptomatic gallstones in middle aged women”, *N Engl J Med*, 321 (1989), 563-9.
- [27] Diehl A.K., “Epidemiology and natural history of gallstone disease”, *Gastroenterol Clin North Am*, 20 (1991), 1-19.
- [28] Dienstag, JA; Isselbacher, KJ. Tumors of the Liver and Biliary Tract. In: Braunwald E, Fauci AS, Kasper DL, et al., editors. *Harrison Principles of Internal Medicine*. 15th International Ed. New Delhi: McGraw Hill; 2001. p. 591.
- [29] Lauga, E. and Stone, H., “Effective slip in pressure-driven Stokes flow”, *J. Fluid Mech.* 489 (2003), 55.
- [30] Gottschalk, M., Lochner, A., “Behaviour of postoperative viscosity of bile fluid from T-drainage. A contribution to cholelithogenesis”, *Gastroenterologisches Journal* 50 (2) (1990), 65-67.
- [31] Coene, P.P.L.O., Groen, A.K., Davids, P.H.P., Hardeman, M.Tytgat, G.N.J., Huibregtse, K., “Bile viscosity in patients with biliary drainage: Effect of co-trimoxazole and N-acetylcysteine and role in stent clogging”, *Scandinavian Journal of Gastroenterology* 29 (1994), 757-763.
- [32] Luo, X.Y., Chin, S.B., Ooi, R.C., Clubb, M., Johnson, A.G., Bird, N., The rheological properties of human bile, *Fourth International Conference on Fluid Mechanics*. Dalian, China (2004).
- [33] Toouli J., “Sphincter of Oddi”, *Gastroenterologist* 4 (1996); 44-53.
- [34] Torsoli A., “Physiology of the human sphincter of Oddi”, *Endoscopy* 20(1) (1988), 166-170.
- [35] Sugita R., Sugimura E., Itoh M., Ohisa T., Takahashi S. and Fujita N., “Pseudolesion of the bile duct caused by flow effect: a diagnostic pitfall of MR cholangiopancreatography”, *Am. J. Roentgenol* 180 (2003), 467-471.
- [36] Toouli J., Dodds W.J., Honda R., Sarna S., Hogan W.J., Komarowski R.A. and Linehan J.H., “Arndorfer RC. Motor function of the opossum sphincter of Oddi”, *J. Clin. Invest.* 71 (1983), 208-220.
- [37] Calabuig R., Ulrich-Baker M.G, Moody F.G. and Weems W.A., “The propulsive behavior of the opossum sphincter of Oddi”, *Am. J. Physiol.* 258 (1990), G138-G142.
- [38] Grivell M.B, Woods C.M, Grivell A.R, Neild T.O, Craig A.G, Toouli J. and Saccone G.T., “The possum sphincter of Oddi pumps or resists flow depending on common bile duct pressure: a multilumen manometry study”, *J. Physiol.*, 558 (2004), 611-622.

- [39] Toouli J., Geenen J.E, Hogan W.J, Dodds W.J and Arndorfer R.C., “Sphincter of Oddi motor activity: a comparison between patients with common bile duct stones and controls”, *Gastroenterology* 82 (1982), 111-117.